RSC Advances

PAPER

View Article Online
View Journal | View Issue

Cite this: *RSC Adv.*, 2017, **7**, 26532

Sequestration of orange G and methylene blue from aqueous solutions using a Co(II) coordination polymer†

Cressa Ria P. Fulong and Timothy R. Cook *

A Co(II) coordination polymer known for its crystalline sponge properties (**CoSP**) is used to sequester Orange G (OG) and methylene blue (MB) in aqueous solutions. Its ability to encapsulate the cationic MB is much greater than for OG. The **CoSP** material is notable for its structural transformations under different conditions (*i.e.* removal from solvent or immersion in alternative solvent systems) giving rise to both 3D and 2D networks. Herein, we study the activated semi-amorphous Co sponge (**a-CoSP**) as a host in aqueous solutions and find that guest uptake results in increased crystallinity as evidenced by powder X-ray diffraction (PXRD). Reactivation releases some dye due to decomposition of the coordination polymer however, the solubility of the building blocks in solution enables the reconstruction of the sponge.

Received 23rd February 2017
Accepted 9th May 2017

DOI: 10.1039/c7ra02286g

rsc.li/rsc-advances

Introduction

Organic dyes are a class of pollutants that are commonly found in industrial wastewater due to their wide application as colorants for textiles, papers, food, and as imaging agents.[1] There are more than 100 000 commercially available organic dyes of various sizes, colors, and ionicity that are being produced annually.[2] Aside from their toxicities and carcinogenicities, these colored effluents may interfere with the absorption and reflection of light in water, thereby affecting biological processes in natural systems.[3] Many dyes are stable and non-biodegradable in water. As a consequence, strict environmental regulations are currently imposed by national and international agencies for the manufacture and use of these organic dyes.[4]

The most common methods for the removal of organic dyes in wastewater is through physical, chemical, and/or biological methods.[5,6] Each method has its own advantages and disadvantages; however, physical removal *via* adsorption is generally considered as the most rapid way to reduce dye concentration in water.[4] Nanomaterials have been extensively studied, not only as adsorbents for the removal of organic dyes in water, but also as photo-catalysts for degradation.[7–11] These materials are very efficient in organic dye removal and degradation but suffer from agglomeration and post-separation difficulties.[2]

Over the past two decades metal–organic frameworks (MOFs) have attracted attention for their application in the adsorption and photo-catalytic degradation of organic dyes.[2,12] One of the practical challenges in the use of MOFs as adsorbents for organic dyes is their water instability.[13] Several studies have demonstrated that frameworks with N-atom donors are more water stable than those with O-atom donors, such as carboxylates.[14,15]

With this in mind, we hypothesized that the $[(Co(NCS)_2)_3(TPT)_4]\cdot 25(o\text{-}C_6H_4Cl_2)\cdot 5(MeOH)$ (TPT = 2,4,6-tris(4-pyridyl)-1,3,5-triazine) "cobalt sponge" coordination polymer (**CoSP**) previously reported by Fujita and co-workers[16] may serve as a stable host for the absorption of organic dyes in water. The host/guest chemistry of this material has been demonstrated using a variety of guests including tetrathiafulvalene,[16] fullerenes,[16] titanocene,[16] aldehydes,[17] and cyclohexanone.[18] This ability of MOFs to accommodate guests in crystalline form was

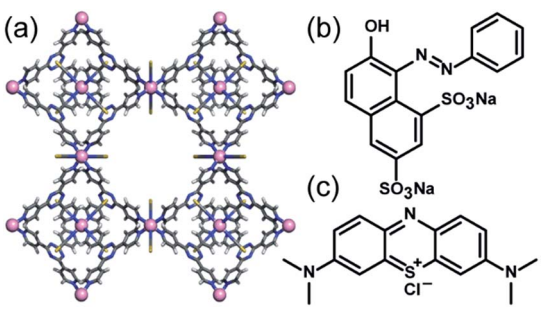

Fig. 1 (a) Structure of **CoSP** (C = gray, N = blue, Co = pink, S = yellow, CCDC no. 766604,† ref. 17); organic dye pollutants orange G (b) and methylene blue (c).

Department of Chemistry, University at Buffalo, The State University of New York, Buffalo, New York 14260, USA. E-mail: trcook@buffalo.edu

† Electronic supplementary information (ESI) available: Experimental details of dye uptake and release; UV-vis spectra; TGA data; PXRD patterns; FT-IR spectra; XPS spectra. See DOI: 10.1039/c7ra02286g

known as the crystalline sponge method. The structure of this Co sponge (Fig. 1a) was initially solved in the cubic space group $Fm\bar{3}m$ with octahedral Co(II) centres with two *trans* NCS ligands and four pyridyl donors originating from four unique TPT ligands. Murugesu and co-workers recently reported microcrystals of **CoSP** belonging to the trigonal space group $R3m$ with the same overall structure as the framework reported by Fujita and co-workers, with different solvents of crystallization.[19] It was observed that the orange crystals (**i-CoSP**; inactive form) transformed to a green semi-amorphous material (**a-CoSP**; activated form) upon removal from the mother liquor, attributed to the removal of solvent and loss of crystallinity of the framework. In this activated form, guest molecules can occupy the void spaces that once housed solvents of crystallization. A second transformation to a 2D network was also observed.[19]

Results and discussion

In this work, the crystalline sponge method for the absorption of an anionic dye, orange G (OG, Fig. 1b), and a cationic dye, methylene blue (MB, Fig. 1c) was investigated. **CoSP** crystals were synthesized in 1 : 1 (v/v) o-$C_6H_4Cl_2$: MeOH as published in the literature.[16] Crystals still immersed in the mother liquor were combined with solutions containing OG or MB. The combined solutions were slowly evaporated to concentrate the dyes.[20] The encapsulation of OG and MB into **i-CoSP** were observed within a few minutes, as shown in videos S1 and S2 (ESI†). The encapsulation process is more distinct with MB, wherein the orange crystals become light green (Fig. 2a and b). Although single crystals were obtained that readily reveal the metal–organic backbone, the location of encapsulated dyes could not be determined due to disorder. The tendency of guests to display static disorder was also observed by Fujita and co-workers.[20]

We were interested in determining if the loss of crystallinity of **CoSP** had an effect on the competency of the material for host/guest chemistry, particularly for organic dyes. The crystalline sponge method is predicated on maintaining single crystal quality, thus the host/guest chemistry of the semi-amorphous state has not been explored. For these experiments, microcrystalline **CoSP** was prepared at a 100 mg scale.[17]

Upon synthesis, orange microcrystals were obtained. Filtration of these microcrystals delivers a fine orange powder (**i-CoSP**, Fig. 2c). Air-drying or activation at 120 °C under vacuum effects a change to a green powder (activated, Fig. 2g).

PXRD patterns of **i-CoSP** (Fig. 3a) and **a-CoSP** (Fig. 3d) are very similar, and also match the pattern of the green semi-amorphous material reported by Murugesu and co-workers. SEM provides further evidence that **a-CoSP** represents a conversion to the semi-amorphous state. The facets observed of the crystallites of **a-CoSP** are softened but still observable in the activated material (Fig. S1†). Our results are consistent with the observations of Murugesu, wherein the transformation into a green powder occurs upon the loss of solvent molecules that occupy voids in the coordination polymer.

Thermogravimetric analysis

TGA curves (Fig. 4) showed three significant mass-loss steps for these materials. The first step at 150 °C is consistent with the removal of H_2O, MeOH, and o-$C_6H_4Cl_2$. The mass-loss at 350 °C has previously been attributed to the decomposition of the TPT ligands.[21]

The final step at 450 °C corresponds to the decomposition of the SCN^- ligands.[19] Both **i-CoSP** and **a-CoSP** showed mass loss as the samples were heated to 150 °C; however, the inactivated sample underwent a larger percent change, consistent with the loss of a greater amount of solvent molecules relative to the activated cage, in which many solvents had already been removed. As the temperature exceeded ~160 °C, a steep drop in % weight was observed attributed to a loss of o-$C_6H_4Cl_2$.

Fourier transform infrared spectroscopy

Fourier transform infrared spectroscopy (FT-IR) analysis further supported the hypothesis of solvent removal upon activation

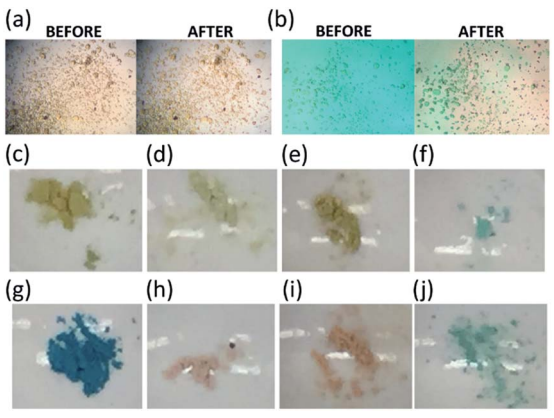

Fig. 2 Images of **CoSP** crystals before and after absorption of (a) OG and (b) MB; (c) **i-CoSP** powder, (d) after adsorption of water, (e) OG, and (f) MB; and (g) **a-CoSP** powder, (h) after adsorption of water, (i) OG, and (j) MB.

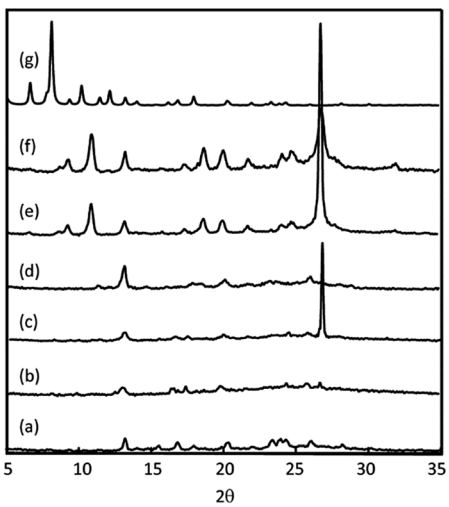

Fig. 3 PXRD patterns of (a) **i-CoSP**; (b) **i-CoSP** + H_2O; (c) **i-CoSP** + aqueous OG; (d) **a-CoSP**; (e) **a-CoSP** + H_2O; (f) **a-CoSP** + aqueous OG; and (g) simulated.

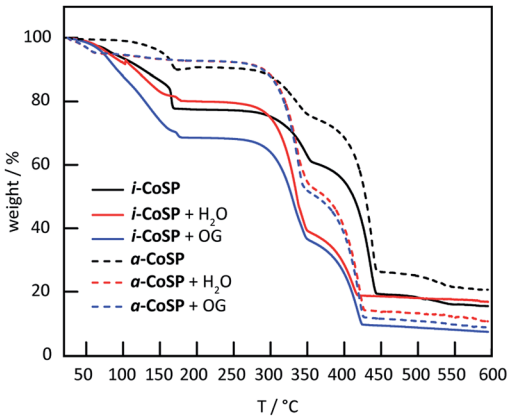

Fig. 4 TGA curves of inactive and activated Co sponge powder before and after uptake of water and OG.

without a total loss of the framework. The FT-IR spectra of both the inactive and activated sponges (Fig. 5) showed characteristic CN stretching bands at <2100 cm^{-1} that correspond to the SCN^- ligands.[22,23]

The broad band at ~3350 cm^{-1} typically observed for OH stretching is absent in both materials. However, stretching (3030 and 1600 cm^{-1}) and bending (690–900 cm^{-1}) bands for the aromatic rings and stretching (800–550 cm^{-1}) bands for C–Cl are observed in **i-CoSP**. These bands are attenuated in **a-CoSP**, as expected if the *o*-$C_6H_4Cl_2$ are removed during activation.

Dye update studies

Both inactive and activated powders were tested for the uptake of OG and MB. ~10 mg of material were added to 40 μM (18 mg L^{-1}) OG and 10 μM (4 mg L^{-1}) MB aqueous solutions. These mixtures were stirred for 30 min at room temperature. The solutions were analysed over the course of 2 days. The electronic absorption spectra showed an 8% decrease in OG concentration for **i-CoSP** and a 55% decrease for **a-CoSP** (Fig. 6a and b). **i-CoSP** removes a significant amount of MB (70% decrease in MB concentration). The use of **a-CoSP** drops the dye concentration even further, by 93% (Fig. 6c and d). Fig. 7 summarizes the absorption capacities (q_e) of 10 mg inactive and activated powders for OG and MB. In all cases, dye uptake is completed within 24 h, resulting in capacities of 0.4 mg g^{-1} for **i-CoSP** + OG; 4.6 mg g^{-1} for **a-CoSP** + OG; 1.4 mg g^{-1} for **i-CoSP** + MB; and 1.8 mg g^{-1} for **a-CoSP** + MB. These values indicate that activation is necessary to maximize the uptake capacity of the Co sponge for both anionic and cationic dyes.

Absorption kinetics

The kinetics of the absorption processes were investigated using a series of absorption experiments (Fig. S2a and b†).[14] The absorption capacities of MB into both **i-CoSP** and **a-CoSP** were plotted against time and the data were fit with first-order kinetics, providing rate constants (k_1) of 0.09 and 0.20 s^{-1}, respectively (Table S1†), indicating that the activated material more rapidly removes the dye from solution. In both cases, the maximum absorption capacity is achieved within 40 minutes. Due to the settling time required for scatter-free spectra, OG uptake was measured every 20 minutes and all spectral changes were complete in the blind-time following initial mixing. Since all uptake occurred within the first 20 minutes, it is clear that OG is sequestered faster than MB.

The ability to remove guests from such systems is attractive insomuch that the material may then be reused to sequester additional molecules.[24] The equilibrium constant associated with the host/guest complexation plays a significant role in the ease with which guests may be removed. The kinetics of the release of OG and MB were investigated (Fig. S2c, d and Table S1†). Using a first-order kinetic model, k_{-1} for dye release was found to be 0.04 s^{-1} for OG. For MB, small spectral changes

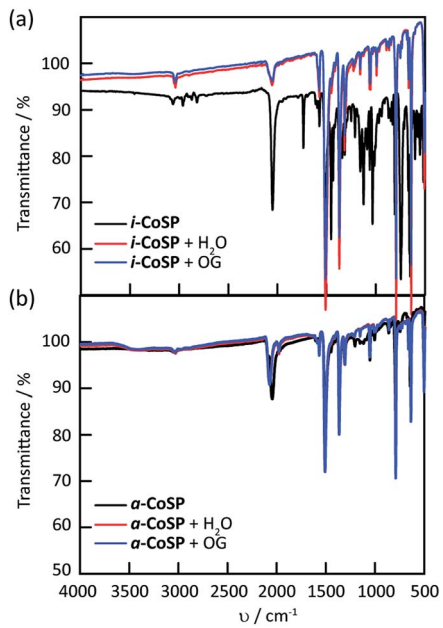

Fig. 5 FT-IR spectra of (a) inactive and (b) activated Co sponge powder before and after uptake of water and OG.

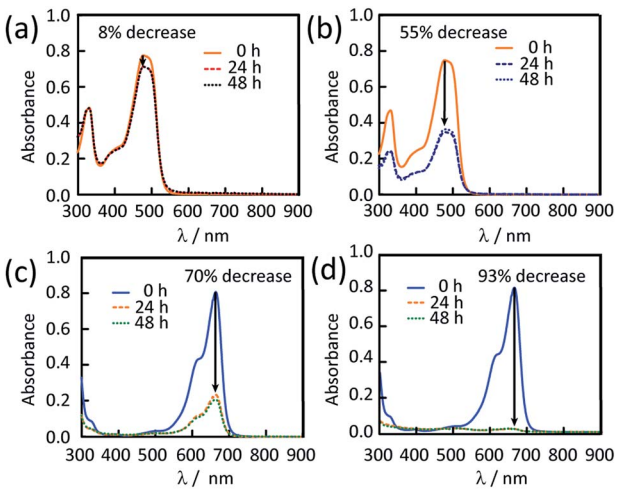

Fig. 6 UV-vis spectra for the dye absorption of **i-CoSP** (left) and **a-CoSP** (right) with OG (top) and MB (bottom).

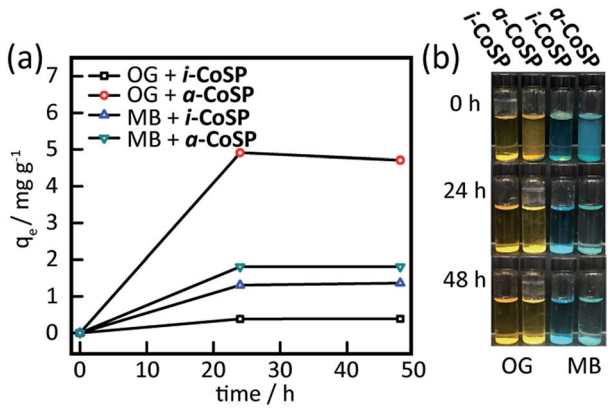

Fig. 7 (a) Absorption capacity (q_e in mg dye per g Co sponge) of inactive and activated Co sponge powder for OG and MB and (b) images of OG and MB solutions after 0, 24, and 48 h of adding inactive and activated Co sponge powder.

were observed when the material was reintroduced to solution; however, these changes are consistent with a small amount of network dissolving and thus releasing the guest, rather than release from the intact **CoSP**. The lack of any significant absorption from free MB obviates a determination of k_{-1} and indicates that MB binds much more strongly to the material.[25]

The water stabilities of **i-CoSP** and **a-CoSP** were determined using UV-vis spectroscopy. **CoSP** has a characteristic band at 500 nm that is used to monitor stability, though the material is very insoluble ($A \sim 0.02$) over the course of 48 hours this band is largely unchanged, with evidence for a slight amount of further dissolution (Fig. S3a and b†). The shoulder at 350 nm is due to absorption by the encapsulated *o*-$C_6H_4Cl_2$ in the inactive material.[26]

X-ray methods

We noted an additional crystal transformation behaviour over the course of our studies. When the semi-amorphous activated powder is exposed to either water or solutions of dyes in water, the PXRD patterns indicate that crystallinity is increased relative to the initial material (Fig. 3). The increase in crystallinity occurs with restoration of solvent molecules back into the coordination network as evidenced by the growth of characteristic bands in the FT-IR spectra (Fig. 5). The presence of encapsulated water is observed as a broad band at 3350 cm^{-1} in the FT-IR spectra (Fig. 5b). Images of the powders, shown in Fig. 2, illustrate that the activated material (Fig. 2g) undergoes a significant colour change when suspended in water (Fig. 2h), or when exposed to the dyes (Fig. 2i and j). Similar changes occur for the inactivated material, however given the orange nature of initial state (Fig. 2c), the changes are subtler. Upon reactivation (**r-CoSP**), *i.e.* activated material is exposed to solvent or dye, then reheated at 120 °C for 10 h, solvent removal is very minimal based on the TGA curves (Fig. S4†) and the PXRD patterns do not show significant differences to those of the singly-activated materials (Fig. S5f and h†). This is consistent with a slow dye release rate wherein dyes largely remain and prevent reuptake. However, **r-CoSP** is still water stable as demonstrated by the minimal decrease in absorption at 500 nm compared to the activated sponge (Fig. S3c†).

X-ray photoelectron spectroscopy (XPS) has been used to provide information about the composition of extended networks and the oxidation states any metal ions present in a sample.[27] XPS was conducted on **a-CoSP**, **a-CoSP** + H_2O, **a-CoSP** + OG, and **a-CoSP** + MB. In all four samples, survey spectra showed the presence of Co(II), N, C, S, and O. The first four components are directly part of the **CoSP** network, whereas the oxygen originates from H_2O or from the dyes, when present. As shown in Fig. S7–S10,† high-resolution peaks corresponding to C 1s indicate a significant amount of non-oxygenated carbon (~284.8 eV) with some C–N contributions at higher energy (~286.9 eV).[28] In all of the samples, the Co 2p binding energies show $2p_{1/2}$ and $2p_{3/2}$ peaks at ~797.2 eV and ~781.2 eV, respectively. These peaks have satellite bands shifted to higher energy by ~6 eV, diagnostic of Co(II).[29,30] Although the bands corresponding to all five elements (Co, N, C, S, O) are present in all samples, the intensities and high resolution fits differ due to the compositional changes associated with activation and guest uptake.

Experimental

Materials and methods

All reagents and solvents were reagent grade and used as received without further purification. 2,4,6-Tris(4-pyridyl)-1,3,5-triazine (TPT), Orange G (OG), and *o*-dichlorobenzene (*o*-$C_6H_4Cl_2$) were purchased from TCI Chemicals. Methylene blue (MB) was purchased from Acros Organics. Cobalt(II) thiocyanate ($Co(NCS)_2$) was purchased from Alfa Aesar. Methanol (MeOH) was purchased from Fisher Chemical. Deionized water was used in all absorption, release, and stability experiments. All UV-vis spectra were acquired from an Agilent Cary 8454 UV-vis Diode Array system with a 10 mm rectangular quartz cuvette. Blank spectra with deionized water were acquired in between runs. All powder X-ray diffraction (PXRD) patterns were collected from a Rigaku Ultima IV system with inert atmosphere attachment and heated sample chamber equipped with Cu source (0.15418 nm Kα) and operated at 1.76 kW power (40 kV, 44 mA). Diffraction patterns were measured within 2θ range of 5 to 35° at a rate of 1° min^{-1}. Thermogravimetric analysis (TGA) curves were measured from a TA Instruments DSC SDT Q600 instrument at a heating rate of 5° min^{-1} from 25–600 °C under constant flow of nitrogen (100 mL min^{-1}). Fourier transform-infrared (FT-IR) spectra were acquired from a Perkin Elmer 1760 FT-IR spectrometer equipped with horizontal attenuated total reflectance (HATR) from 4000 to 500 cm^{-1} wavenumbers. Field Emission Scanning Microscope (FESEM) images were captured using a Hitachi SU70 FESEM with Oxford Energy-dispersive X-ray Spectrometer (EDS). All X-ray photoelectron spectroscopy (XPS) spectra were measured using a Physical Electronics Phi Versaprobe 5000 with Al Kα source instrument.

Syntheses

Synthesis of crystalline Co sponge (CoSP). Co sponge crystals, $\{[(Co(NCS)_2)_3(TPT)_4]\cdot 25(o\text{-}C_6H_4Cl_2)\cdot 5(MeOH)\}_n$, were grown

following a published procedure.[16] A solution of TPT (6.3 mg, 20 μmol) in 5 mL of 1 : 4 (v/v) MeOH : *o*-$C_6H_4Cl_2$ was placed in a dram vial. Carefully layered on top of this is a 1 mL MeOH solution of $Co(NCS)_2$ (7.0 mg, 40 μmol). This solution was left to stand for 7 days or until orange crystals are formed on the glass surface.

Synthesis of inactive Co sponge powder (i-CoSP). $\{[(Co(NCS)_2)_3(\kappa^3\text{-TPT})_4]\cdot a(H_2O)\cdot b(MeOH)\}_n$ (**i-CoSP**),[19] was synthesized following a published procedure.[17] A solution of TPT (315 mg, 1.0 mmol) in 250 mL of 1 : 4 (v/v) MeOH : *o*-$C_6H_4Cl_2$ was placed in a 500 mL round bottom flask and stirred at 600 rpm. A 50 mL MeOH solution of $Co(NCS)_2$ (350 mg, 2.0 mmol) was added to the TPT solution. The mixture was stirred for 15 min and left to stand for 2 h. **i-CoSP** was collected by filtration and washed with *o*-$C_6H_4Cl_2$.

Activated Co sponge powder (a-CoSP). $\{[(Co(NCS)_2)_3(\kappa^{0-3}\text{-TPT})_4]\cdot c(H_2O)\}_n$[19] (**a-CoSP**) was prepared by pre-treating the synthesized powder before use.[31] This involves heating the synthesized **i-CoSP** at 120 °C under vacuum for at least 10 h.

Conclusions

In summary, we have established that **CoSP** MOF first reported by Fujita and co-workers is capable of serving as a host for two organic dyes, OG and MB. The absorption capability of the sponge is greatly enhanced by removal of trapped solvents by activating with heat at 120 °C for 10 h. The activation accelerates the transformation to a semi-amorphous material previously discovered by Murugesu and co-workers. We have shown that this activation altered the crystallinity of the MOF but does not hinder host/guest chemistry. Removal of trapped solvents frees up void spaces for dye encapsulation. **CoSP** does not degrade in aqueous solution and remains capable of dye adsorption even in a semi-amorphous state. The crystallinity of the material was greatly affected by this host/guest chemistry. The semi-amorphous activated form regained crystallinity when immersed in water or solutions of dyes. Although the kinetics of uptake were faster for OG, the cationic MB bound much more tightly to the framework, with minimal reversibility.

Acknowledgements

TRC thanks the University at Buffalo and State University of New York Research Foundation for support. The authors thank Dr Joshua Wallace for assistance with XPS measurements.

Notes and references

1 G. Booth, H. Zollinger, K. McLaren, W. G. Sharples and A. Westwell, in *Ullmann's Encyclopedia of Industrial Chemistry*, Wiley-VCH Verlag GmbH & Co. KGaA, 2000, DOI: 10.1002/14356007.a09_073.
2 C.-C. Wang, J.-R. Li, X.-L. Lv, Y.-Q. Zhang and G. Guo, *Energy Environ. Sci.*, 2014, **7**, 2831–2867.
3 W.-T. Tsai, H.-C. Hsu, T.-Y. Su, K.-Y. Lin, C.-M. Lin and T.-H. Dai, *J. Hazard. Mater.*, 2007, **147**, 1056–1062.
4 *Environmental Chemistry of Dyes and Pigments*, ed. A. F. Reife and H. S. Freeman, John Wiley and Sons, New York, 1996.
5 O. J. Hao, H. Kim and P.-C. Chiang, *Crit. Rev. Environ. Sci. Technol.*, 2000, **30**, 449–505.
6 Y. M. Slokar and A. Majcen Le Marechal, *Dyes Pigm.*, 1998, **37**, 335–356.
7 S. Wang, H. Sun, H. M. Ang and M. O. Tadé, *Chem. Eng. J.*, 2013, **226**, 336–347.
8 S. C. N. Tang and I. M. C. Lo, *Water Res.*, 2013, **47**, 2613–2632.
9 X. Wang, M. Zhu, H. Liu, J. Ma and F. Li, *Sci. Total Environ.*, 2013, **449**, 157–167.
10 X. Zhao, L. Lv, B. Pan, W. Zhang, S. Zhang and Q. Zhang, *Chem. Eng. J.*, 2011, **170**, 381–394.
11 D. Shuai, D. C. McCalman, J. K. Choe, J. R. Shapley, W. F. Schneider and C. J. Werth, *ACS Catal.*, 2013, **3**, 453–463.
12 E. M. Dias and C. Petit, *J. Mater. Chem. A*, 2015, **3**, 22484–22506.
13 A. Ayati, M. N. Shahrak, B. Tanhaei and M. Sillanpää, *Chemosphere*, 2016, **160**, 30–44.
14 Z.-P. Qi, J.-M. Yang, Y.-S. Kang, F. Guo and W.-Y. Sun, *Dalton Trans.*, 2016, **45**, 8753–8759.
15 J. J. Low, A. I. Benin, P. Jakubczak, J. F. Abrahamian, S. A. Faheem and R. R. Willis, *J. Am. Chem. Soc.*, 2009, **131**, 15834–15842.
16 Y. Inokuma, T. Arai and M. Fujita, *Nat. Chem.*, 2010, **2**, 780–783.
17 S. Matsuzaki, T. Arai, K. Ikemoto, Y. Inokuma and M. Fujita, *J. Am. Chem. Soc.*, 2014, **136**, 17899–17901.
18 Y. Y. Inokuma Shota, A. Junko, A. Tatsuhiko, H. Yuki, T. Kentaro, M. Shigeki, R. Kari and F. Makoto, *Nature*, 2013, **495**, 461–466.
19 G. Brunet, D. A. Safin, I. Korobkov, A. Cognigni and M. Murugesu, *Cryst. Growth Des.*, 2016, **16**, 4043–4050.
20 M. Hoshino, A. Khutia, H. Xing, Y. Inokuma and M. Fujita, *IUCrJ*, 2016, **3**, 139–151.
21 M.-X. Li, Z.-X. Miao, M. Shao, S.-W. Liang and S.-R. Zhu, *Inorg. Chem.*, 2008, **47**, 4481–4489.
22 K. Nakamoto, in *Infrared and Raman Spectra of Inorganic and Coordination Compounds*, John Wiley & Sons, Inc., 2008, ch. 2, pp. 149–354, DOI: 10.1002/9780470405840.
23 B. Schrader, in *Infrared and Raman Spectroscopy*, Wiley-VCH Verlag GmbH, 2007, pp. 711–764, DOI: 10.1002/9783527615438.refs.
24 S.-N. Sheng, Y. Han, B. Wang, C. Zhao, F. Yang, M.-J. Zhao, Y.-B. Xie and J.-R. Li, *J. Solid State Chem.*, 2016, **233**, 143–149.
25 M. Roushani, Z. Saedi and T. Musa beygi, *J. Taiwan Inst. Chem. Eng.*, 2016, **66**, 164–171.
26 J. G. Mattay and A. G. Griesbeck, in *Photochemical Key Steps in Organic Synthesis*, Wiley-VCH Verlag GmbH, 2007, pp. 261–283, DOI: 10.1002/9783527615797.ch05.
27 J. Jiang, L. Huang, X. Liu and L. Ai, *ACS Appl. Mater. Interfaces*, 2017, **9**, 7193–7201.
28 S. Bag, K. Roy, C. S. Gopinath and C. R. Raj, *ACS Appl. Mater. Interfaces*, 2014, **6**, 2692–2699.
29 W. Wei, W. Chen and D. G. Ivey, *Chem. Mater.*, 2008, **20**, 1941–1947.
30 S. Bennici, H. Yu, E. Obeid and A. Auroux, *Int. J. Hydrogen Energy*, 2011, **36**, 7431–7442.
31 F.-R. Dai, D. C. Becht and Z. Wang, *Chem. Commun.*, 2014, **50**, 5385–5387.

